The Thesis Committee for Tien-Yu Huang
Certifies that this is the approved version of the following thesis:

Interactive roles of core clock components and histone methyltransferases in circadian chromatin regulation in Arabidopsis

APPROVED BY
SUPERVISING COMMITTEE:

Supervisor:

Jeffrey Chen

Hong Qiao

Interactive roles of core clock components and histone methyltransferases in circadian chromatin regulation in Arabidopsis

by

Tien-Yu Huang, B.S.; M.S.

Thesis

Presented to the Faculty of the Graduate School of

The University of Texas at Austin

in Partial Fulfillment

of the Requirements

for the Degree of

Master of Arts

The University of Texas at Austin

December 2016

Abstract

Interactive roles of core clock components and histone methyltransferases in circadian chromatin regulation in Arabidopsis

Tien-Yu Huang, M.A.

The University of Texas at Austin, 2016

Supervisor: Jeffrey Chen

The importance of circadian clock function has been demonstrated in almost all organisms examined to date. Despite divergences in oscillator components, a chromatin-dependent mechanism of clock gene regulation appears to be common in the circadian system among different organisms. Previous studies have shown that rhythmic expression of core clock components correlates with circadian oscillations of active chromatin markers at the promoters. In this study, we investigate the time-dependent pattern of activating chromatin marks H3K4me3 and H3K9ac on a genomic scale to identify genes with a circadian chromatin profile in Arabidopsis. We found that about one fourth of loci with H3K4me3 occupancy or H3K9ac occupancy showed a rhythmic chromatin oscillation. We further identified that the H3K4me3 methyltransferases Arabidopsis Thaliana Trithorax Protein 1 (ATX1) and the Arabidopsis ASH1 HOMOLOG 2 (ASHH2) are subjected to clock control. In addition, ASHH2 was shown to be a novel regulator of core clock genes. Our findings propose a functional link between core clock regulators and temporal modification of activating chromatin marks in plant.

Table of Contents

List of Figures

Introduction

Several studies have shown the connection between chromatin remodeling and the circadian clock in animal [1-4]. Rhythmic H3 acetylation have been shown to be associated with the cyclic transcription of several clock-controlled genes, including Period 1, 2 and 3 (Per1, Per2 and Per3) and Cryptochromes 1 and 2 (Cry1 and Cry2) [5-7]. The transcriptional activator CLOCK was demonstrated to possess intrinsic HAT activity and is able to associate with the NAD+-dependent histone deacetylase SIRT1 to control the deacetylation of both H3 and BMAL1 [8-10]. Per1 was shown to interact with WDR5, a component of histone methyltransferase (HMT) complex, to mediate rhythmic k4 and k9 methylation at the promoters of Per1-regulated genes [11]. In addition, the mammalian homolog of Drosophila trithorax Mixed lineage leukemia 1 (MLL1) is shown to form a complex with CLOCK–BMAL1 and contributes to its rhythmic recruitment to circadian promoters and to H3 acetylation [12]. These findings suggested a crucial role of dynamic histone modifications in both fine-tuning of clock activity and in collaborating with clock to mediate downstream gene expression.

In Arabidopsis, the rhythmic expression of several circadian clock genes including LHY, CCA1, TOC1, PRR9, PRR7 and LUX correlates with oscillating acetylation at H3K9, H3K14 and H3K56, as well as tri-methylation at H3K4. [13-17]. Histone acetylation and tri-methylation at H3K4 are active marks that contribute to both the magnitude and periodicity of core clock gene transcription [18]. On the other hand, only a few histone modifiers, including HMT, histone demethylase (HDM), and histone deacetylase (HDAC), have been suggested to play a partial role in the regulation of circadian gene expression [16, 19, 20]. Given the importance of dynamic histone

modification in coordinating gene expression, gene networks contribute to the oscillating acetylation and methylation in *Arabidopsis* remain largely unclear. Furthermore, a comprehensive study of the dynamic histone modifications in circadian condition is still lacking.

Circadian regulation of active chromatin markers

Based on observations that clock loci undergo changes in chromatin state over the circadian cycle, we hypothesized that this might be more generally applicable on a genomic scale. We investigated this by performing chromatin immunoprecipitation (ChIP) and high-throughput sequencing (ChIP-seq) on 14d Arabidopsis rosette leafs over the circadian cycle to delineate global changes in the active epigenome H3K4me3 and H3K9ac over a 24-h time frame. We focused on the circadian profile of H3K4me3 and H3K9ac on a genomic scale. Using the non-parametric rhythmicity detecting algorithm JTK_CYCLE [21], we were able to identify loci with cycling of H3K4me3 or H3K9ac chromatin marks. The results showed that about 25% (4181/16618) of loci with H3K4me4 binding signals and about 23% of (5318/22661) loci with H3K9ac binding signals exhibited cycling patterns of activating chromatin marks (Fig. 1A, 1B). The phase distribution analysis showed that the majority of loci with cyclic H3K4me3 binding peak around early day, while those with cyclic H3K9ac binding patterns span around the night and early morning (Fig. 1C, 1D). These findings correlated well with the previous report that a significant portion of loci display cyclic alternation of H3K4me3 and H3K9ac binding profiles, while the two active marks have distinct mean circular phases [22].

The differential pattern of accumulation and the differences in peak phases implicate specific roles for H3K4me3 and H3K9ac in chromatin architecture at different times of the day. To further investigate the role each of them played, we clustered the loci with cyclic binding profiles of H3K4me3 and H3K9ac into two major categories, morning and evening phase, using k-medoids algorithm (Fig. 1A, 1B). The morning and evening clusters of each active chromatin mark are showed in the heatmap. Direct comparison of the evening-phased H3K4me3 loci (2254) with H3K9ac loci (2883) revealed that only 469 loci are common to both groups (Fig. 1E). Similarly, only 339 loci are common to both the morning-phased H3K4me3 (1926) and H3K9ac loci (2434) (Fig. 1F). The results from gene ontology analysis further showed a differential enrichment of GO categories in the morning and evening clusters of H3K4me3 and H3K9ac (Fig. s1). These results supported the idea of distinct roles of H3K4me3 and H3K9ac in circadian regulation of chromatin status on target genes.

We next examined the relevance of the oscillating chromatin changes for rhythmic gene expression. Initially, we cross-correlated rhythmic H3K4me3- and H3K9ac-binding sites with genes that had been shown previously to be rhythmic by gene expression profiling [23]. As shown in the heatmap and phase distribution charts, the majority of genes clustered as morning phase based on their H3K4me3- and H3K9ac-binding profiles also demonstrated a morning-phased transcriptome expression, which indicated a strong correlation between circadian chromatin modifications with corresponding gene expressions on a genome-wide scale (Fig. s2A, s2B)(Fig. 1G, 1H). A similar phenomenon can be observed in the evening-phased H3K4me3 and H3K9ac clusters.

Interactive roles of core clock components with histone modifications

The rhythmic expression of core clock genes LHY, CCA1, and TOC1 have been shown to correlate with oscillating active chromatin modifications. We examined the status of H3K4me3 and H3K9ac on core clock genes from our genome-wide ChIP-Seq data to validate the previous findings. The ChIP binding signals are normalized and displayed in the IGV genome browser. Both H3K4me3 and H3K9ac exhibited a clear circadian profile at the promoter region of core clock loci (Fig. 2A, 2B). Quantification of the binding signals confirmed that morning-expressed oscillator genes LHY and CCA1 exhibited peak expression of H3K4me3 and H3K9ac at ZT3 and ZT0, respectively, compared to the evening-expressed oscillator genes TOC1, which has a peak expression of H3K4me3 and H3K9ac at ZT15 and ZT12 (Fig. 2C, 2D). The transcript levels of LHY, CCA1, and TOC1 showed a strong correlation with H3K4me3 and H3K9ac expressions on a diurnal basis. These results coincide with the previous findings that the rhythms in H3K9ac and H3K4me3 correlate with gene expressions of core clock loci while phase of H3K4me3 was delayed with a peak a few hours later compared with the peak of H3K9ac accumulation [24].

It has been shown previously that the core clock proteins regulate the activity of target genes by directly alerting their promoter chromatin status [12]. To investigate whether a similar relation exists on a genome-wide scale, we pulled out the direct targets of CCA1, TOC1, PRR5 and PRR7 from previously published dataset, and compared the enrichment levels of core clock target genes in the morning and evening clusters [25-27]. The results showed that about 34 % and 28% of TOC1 targets with rhythmic transcript expression (> 0.75 MBPMA in LL (LL23_LDHH)) have morning-phased cyclic H3K4me3- and H3K9ac- binding patterns, respectively, while only less than 17% of

TOC1 targets could be found in the evening-phased cluster (Fig. 2E). This finding correlated well with the previously identified role of TOC1 being an inhibitor in the expression of its target genes [26]. In addition, we found about 33% and 30 % of rhythmic CCA1 targets genes in the evening cluster of loci with rhythmic H3K4me3- and H3K9ac-binding patterns, respectively (Fig. 2F). The results support the role of CCA1 as majorly an inhibitor in the regulation of downstream target genes, while the interplay between different core clock components could make its effect on clock targets more complicate [25]. The comparison of PRR5 and PRR7 targets with the morning and evening clusters showed a similar trend as in TOC1 (Fig. s3A, s3B), which implicated a similar role among the PRR family as an inhibitor to their targets[28]. Together, these results suggested that the core clock components could contribute directly in the regulation of cyclic modification of active chromatin marks.

Regulation of active chromatin status by core clock components

Next, we sought to explore the details of how the core clock components could control rhythmic chromatin modifications on a genome-wide scale. In the animal model, active H3K4me3 histone methyltransferases Mixed Lineage Leukemia 1 (MLL1) and Mixed Lineage Leukemia 3 (MLL3) have been shown to interact directly with core clock components or be regulated by clock, respectively, to contribute to genome-scale circadian transcription [12, 29]. To examine if a similar regulatory mechanism exists in Arabidopsis, we assayed the expression in members of the SET Domain Group (SDG) with confirmed H3K4 trimethylation activity. The results showed that only the Arabidopsis Thaliana Trithorax Protein 1 (ATX1) and the Arabidopsis ASH1 HOMOLOG 2 (ASHH2) showed rhythmic abundance over the circadian cycle, with peak

expression at the early morning (Fig. s4). The expression of ATX1 and ASHH2 were disrupted in a *cca1/lhy* double mutant background, which indicates that both histone methyltransferases are subjected to clock control (Fig. s4). We further confirmed this phenomenon by performing a luciferase assay with ATX1::LUC and ASHH2::LUC reporters in wildtype (WS) and double mutant (*cca1/lhy*) background. The results showed that the promoter activities and periodicity of histone methylatransferases ATX1 and ASHH2 were altered in the clock mutant background, which are consistent with the expression data (Fig. 3A-D). Together, these findings suggested that the expression levels of histone methylatransferases ATX1 and ASHH2 are regulated by core clock.

To further characterize the role of core clock proteins in the regulation of H3K4me3 level on a genome wide scale, we performed ChIP-seq on 14d Arabidopsis rosette leafs collected from wildtype (WS) and double mutant (*cca1/lhy*) at ZT0 and ZT12. The results showed a loss of trimethylation on loci with H3K4me3 binding signals at ZT0 (Fig. 3E). Interestingly, the loss of trimethylation of H3K4 was diminished at ZT12, which indicates a temporal effect of core clock protein CCA1 and LHY on genome wide H3K4me3 level (Fig. 3F). A comparison between CCA1 LD binding targets (919) and the loci with decreased H3K4me3 levels in double mutant at ZT0 (806) showed that only 48 genes are common to both groups. This suggested that the majority of loci with decreased H3K4me3 levels at ZT0 are not directly controlled by CCA1, whereas the core clock can modulate genome wide temporal H3K4me3 levels by regulating the expression of K4 trimethylation methylatransferases. Thus, histone methylatransferases ATX1 and ASHH2 are clock-controlled factors that could potentially regulate the circadian epigenomic profiles in plant.

Regulation of clock by K4 trimethylation methylatransferases

ATX1 and ASHH2 are versatile regulators in *Arabidopsis*, participating in pathways such as development, flowering time, plant immunity and light responsive reaction [30-33]. Their role in the light responsive pathway suggested that these histone methylatransferases could be a potential regulator of core clock genes. To address this question, we checked the transcript levels of core clock components in the mutant lines *atx1* and *ashh2*. We found that the amplitudes of expression of CCA1 and TOC1 were significantly altered in *ashh2* compared to wildtype (Fig. 4A). On the contrary, none of the clock components showed a significant difference in expression in *atx1* mutant. The role of ATX1 in the regulation of clock could be complexed by the existence of ATX1 duplicated gene ATX2 in *Arabidopsis*. To further confirm the effect of the mutant *ashh2* on clock genes, we established transgenic lines expressing CCA1::Luc and examined the promoter activity of CCA1 in *ashh2* mutant under constant condition. The results confirmed our expression data that both the rhythmicity and amplitude of CCA1 promoter activities were significantly altered in *ashh2* plants (Fig. 4B, 4C). In addition, the chromatin status of CCA1 and TOC1 displayed variation in H3K4me3 levels, which coincide well with the reporter and transcript expressions (Fig. 4D). These findings suggested an important role of histone methylatransferase ASHH2 in the regulation of core clock genes, which could potentially coordinate the interaction between light responsive pathway and circadian clock regulation (Fig. 4E).

A recent study using transgenic plants expressing recombinant protein to identify genes directly bound by ASHH2 showed that the PSEUDO-RESPONSE REGULATOR 9 (PRR9), a morning-expressed member of the PRR family, is a direct target of ASHH2 [33]. This finding indicated that histone methylatransferase ASHH2 can coordinate clock

expression by directly targeting morning-expressed PRR9. The expression of CCA1 and TOC1 could, therefore, be indirectly regulated by ASHH2. It is worth mentioning that by doing a phase distribution analysis of the targets of ASHH2, we found that the majority of them are early morning-phased, which is very similar to the phase distribution of TOC1 targets (Fig. s6). This suggested that the activity and expression of ASHH2 is tightly regulated temporally, which could be due to its role in both light responsive pathway and circadian clock regulation.

In this study, our findings indicated that a forth of loci with activating chromatin mark H3K4me3 or H3K9ac enrichment underwent rhythmic oscillation of activating chromatin levels. Although both H3K4me3 and H3K9ac are strongly correlated with gene activation, the gene sets with cyclic H3K4me3 marks or cyclic H3K9ac marks are distinct, indicating the special roles and functions of each mark at temporal chromatin modification. We further showed that the core clock components could contribute in the circadian changes of H3K4me3 levels by modulating the expression of K4 trimethylation methylatransferases ATX1 and ASHH2. The results from previously published datasets suggested that the genic region of ATX1 and ASHH2 are not direct targets of CCA1 or TOC1 protein. Thus, the mechanism of how the clock mutant influences the expression ATX1 and ASHH2 require further investigation. It is possible that other core clock genes could target ATX1 and ASHH2 directly, given the fact that the promoters of these two genes harbor circadian elements. Interestingly, it has been shown that ATX1 and ASHH2 can formed a complex potentially, which was postulated as a plant ortholog of the trithorax group (trxG) complexe in animal [34]. The trxG complexes are involved in the formation of an open chromatin structure that promotes an active epigenetic modification at specific promoters. In addition, previous findings also shown that MLL1 and MLL3,

the two histone methyltransferase mediate oscillation of circadian gene expression in mouse model, are trxG complexe proteins [35]. These results along with our findings in this study implicated a conserved role of the trxG complexe in participating in clock regulation and in clock-mediated control of physiological pathways.

Methods

Plant Materials

Plant materials include the following A. thaliana ecotypes Columbia (Col) and Ws. Crossing was carried out as previously described [36]. The *cca1-11lhy21* (CS9380) T-DNA insertion mutants in the Ws background and *ashh2-2* (SALK_026442) T-DNA insertion mutants in the Col background were obtained from the Arabidopsis Biological Resource Center (ABRC). The *atx1-1* insertion mutant is a kindly provided by Professor Zoya Avramova. All plants were grown under a 16/8-h light/dark cycle with temperatures of 22 °C (light) and 20 °C (dark) on soil, and rosette leaves from ~2-week-old plants before flowering were collected for RNA analysis, unless otherwise noted. For qRT–PCR validation, plants were grown in three biological replicates, and leaves were harvested every 4 h for two diurnal cycles (48 h). For plant transformation, 4- to 5-week-old plants were used for *Agrobacterium tumefaciens*-mediated transformation through floral dipping [37].

ChIP and template preparation for Illumina sequencing analysis

Chromatin immunoprecipitation (ChIP) was performed using mature leaves (~3 g) of A. thaliana (Col) following the published protocol as described in [38]. For immunoprecipitation, antibodies against H3K4me3 (Ab8580), and H3K9ac (Ab10812),

respectively, were added to a 600-μL solution containing diluted chromatin extracts and incubated overnight at 4°C with gentle rotation. Immunoprecipitated chromatin-DNA (IP-DNA) and 50 μL of input chromatin-DNA (without IP) were subjected to reverse cross-link and purified for sequencing libraries preparation. ChIP-seq libraries were constructed according to protocols described in the Illumina ChIP sequencing kit (Illumina Inc.). DNA fragments with a range of 250–300 bp were excised and amplified for subsequent cluster generation and massively parallel sequencing.

Sequence read mapping and identification of nucleosomes in A. thaliana genome

The sequence reads (40–60 bp) were aligned to the A. thaliana genome (version TAIR10) as described in [39]. The steps of sequencing depth selection, quality checking, mapping, data normalization, assessment of reproducibility, peak calling, differential binding analysis, controlling the false discovery rate, peak annotation generally followed the procedures described in [40].

Bioinformatics analyses

Differentially expressed genes were identified using the MACS2 with a log10 likelihood > |2| and a FDR-corrected P value (q value) < 0.05 [41]. Heat maps were generated and clustering was performed using the R. GO analysis was performed and figures were generated using the agriGO website [42]. The hypergeometric test was used to identify enriched (FDR-adjusted P value < 0.05) GO categories relative to the genome background. The non-parametric algorithm JTK_CYCLE was used to detect rhythmic components in genome-scale datasets [21].

RNA extraction and qRT–PCR

Tissue collected for gene expression analysis was from plants before bolting (2-week-old plants unless noted otherwise) at indicated ZT (ZT0=dawn). Total RNA was extracted using Concert Plant RNA Reagent (Invitrogen) and digested with RQ1 RNase-Free DNase (Promega) according to the manufacturer's instructions. cDNA was synthesized using 1 μM oligo dT (12–18) primer (GeneLink) from 1 μg DNase-treated RNA using the Omniscript RT Kit (Qiagen) according to the manufacturer's instructions. For qRT–PCR, FastStart Universal SYBR Green Master (Rox; Roche Applied Science) was used for PCR in the presence of gene-specific primers and 2 μl of diluted cDNA template. Expression levels of target genes were normalized against transcript levels of ACT7 (At5g09810) and relative expression levels of transcripts were calculated.

Luciferase assays

Plants containing either ATX1:LUC or ASHH2:LUC constructs were analysed using a Packard TopCount luminometer as previously described [43]. Seeds were sterilized with bleach and 75% ethanol and plated on 1% (w/v) agar with MS media containing 7.5 mg l−1 phosphinothricin. Seeds were stratified 2 days in the dark at 4 °C and then transferred into 16-h light and 8-h dark cycles for 7 days, and then transferred to MS containing no selection for 3 days. Seedlings were transferred to white microtitre plates (Nunc, Denmark) containing agar MS medium plus 30 g sucrose/L and 30 μl of 0.5 mM luciferin (Gold Biotechnology). Microtitre plates were covered with clear plastic MicroAmp sealing film (Applied Biosystems, Foster City, CA) in which holes were placed above each well for seedling gas exchange. One day after addition of luciferin, plates were moved to the TopCount and interleaved with two clear plates to allow light diffusion to the seedlings. All luciferase data were analysed using the Biological Rhythm Analysis Software System (www.amillar.org). All period estimates were performed on

rhythms from 24 to 120 h using fast Fourier transform–nonlinear least squares (FFT–NLLS) analysis [44].

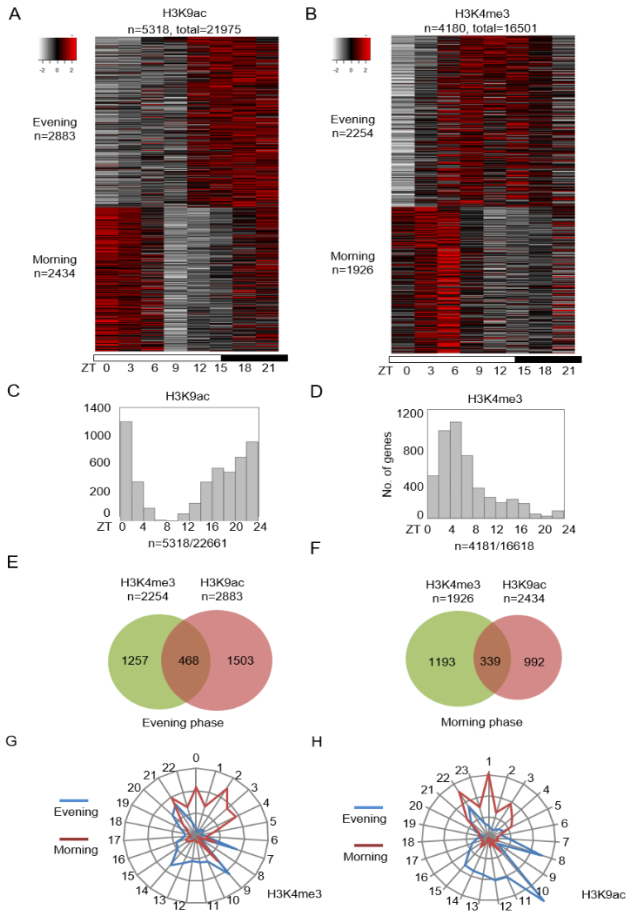

Figure 1: Diurnal regulation of histone modifications in Arabidopsis thaliana. (**A**) (**B**) Heat-map view of H3K4me3 (A) and H3K9ac (B) binding signals of cyclic peaks at ZT0 to ZT21 (3-hour interval), from –1kb to +1 kb surrounding the center of TSS. The signals are partitioned into the morning and evening clusters around medoids using R. The number of total peaks and the number of peaks in each cluster are indicated at the top or left side of the panel. (**C**) Histograms showing circadian phase distributions of genes with rhythmic H3K9ac signal. Cyclic binding was determined by JTK cycling ($p < 0.05$). The x axis represents the estimated phases obtained from JTK cycling. **(D)** Histograms showing circadian phase distributions of genes with rhythmic H3K4me3 signal. Cyclic binding was determined by JTK cycling. The x axis represents the estimated phases obtained from JTK cycling. (**E**) Venn diagram of genes with evening-phase cyclic H3K4me3 and H3K9ac signals. (**F**) Venn diagram of genes with morning-phase cyclic H3K4me3 and H3K9ac signals. (**G**) **(H**) The phase distribution of genes with cyclic H3K9ac (E) or H3K4me3 (F) binding signals. The blue line and red line represent loci clustered as evening phase or morning phase, respectively.

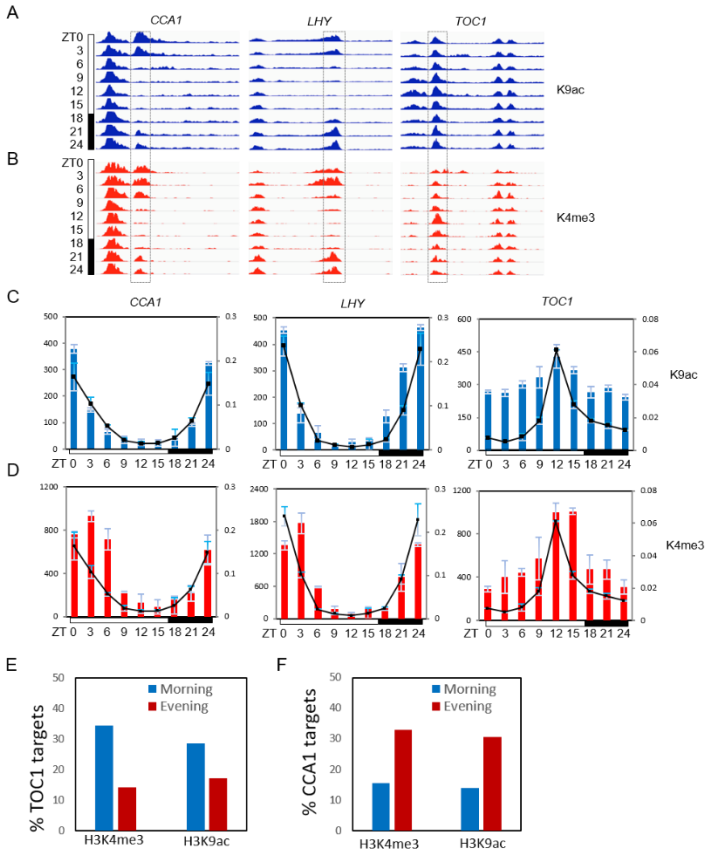

Figure 2: Interactive roles of the clock regulators and histone modifications in gene expression. (**A**) (**B**) Genomic browser view of H3K4me3 (A) and H3K9ac (B) occupancy at the core clock components CCA1, LHY and TOC1 at different ZTs. Each track represents the normalized ChIP-seq read coverage at a single time point. The y axis scales are identical for all three genes. (**C**) (**D**) Quantifications of the ChIP-seq signal as presented in (A) and (B), respectively. The x axis indicates the reads number measured over 100-bp fragment encompassing the +/-1000 bp region of the transcription start site. Expression profiling for each gene is overlapped in each graph (black line). mRNA abundance was normalized to ACT7 expression. Values are represented as means ± SEM. (**E**) Bar graph of enrichment in rhythmic TOC1 targets in genes with cyclic chromatin binding signals. TOC1 binding targets are pulled from previously published data set. Y axis is the percentage of binding loci identified as having cyclic H3K4me3 or H3K9ac binding signals. (**F**) Bar graph of enrichment in rhythmic CCA1 targets in genes with cyclic chromatin binding signals. CCA1 binding targets are pulled from previously published data set. Y axis is the percentage of CCA1 binding loci identified as having cyclic H3K4me3 or H3K9ac binding signals.

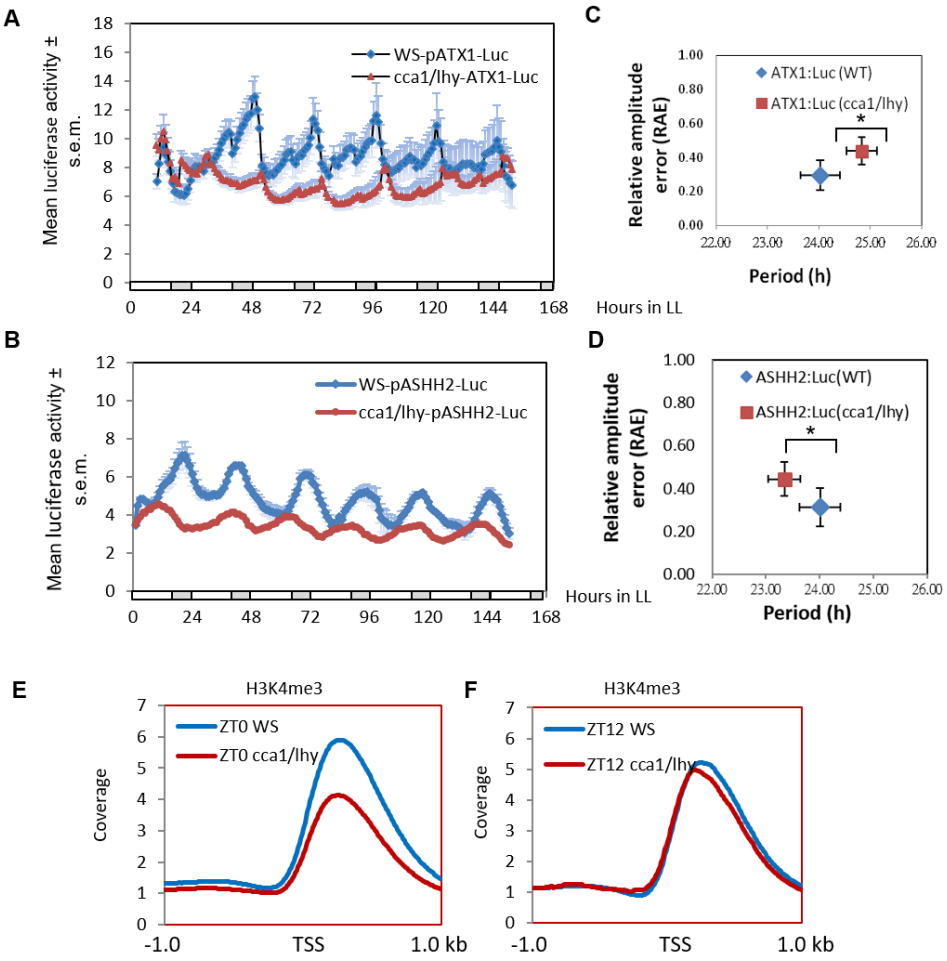

Figure 3: The clock regulates the expression and periocity of histone methyltransferases. (**A**) and (**C**) Bioluminescence analysis of ATX1::LUC (A) and ASHH2::LUC (C) expression in T-DNA insertion line cca1/lhy and in wt. (C) (n >25 seedlings per genotype) Wild-type (wt) traces correspond to ATX1::LUC (A) or ASHH2::LUC (C) seedlings, respectively. (**B**) and (**D**) Phase change of luciferase expression in wild-type ATX1::LUC (wt) (B) or ASHH2::LUC (wt) (D) and in the clock double mutant ATX1::LUC (cca1/lhy) (B) or ASHH2::LUC (cca1/lhy) (D) as shown in (A) and (C), respectively. Each symbol represents the normalized phase from n > 25 seedlings. (**E**) (**F**) Binding profiles of H3K4me3 at the TSS +/- 1kb.in wild-type (WS) and clock double mutant (cca1/lhy) at ZT0 (E) and ZT12(F), respectively. The y axis represents the average signal in a 100-bp bin (normalized uniquely mapped reads).

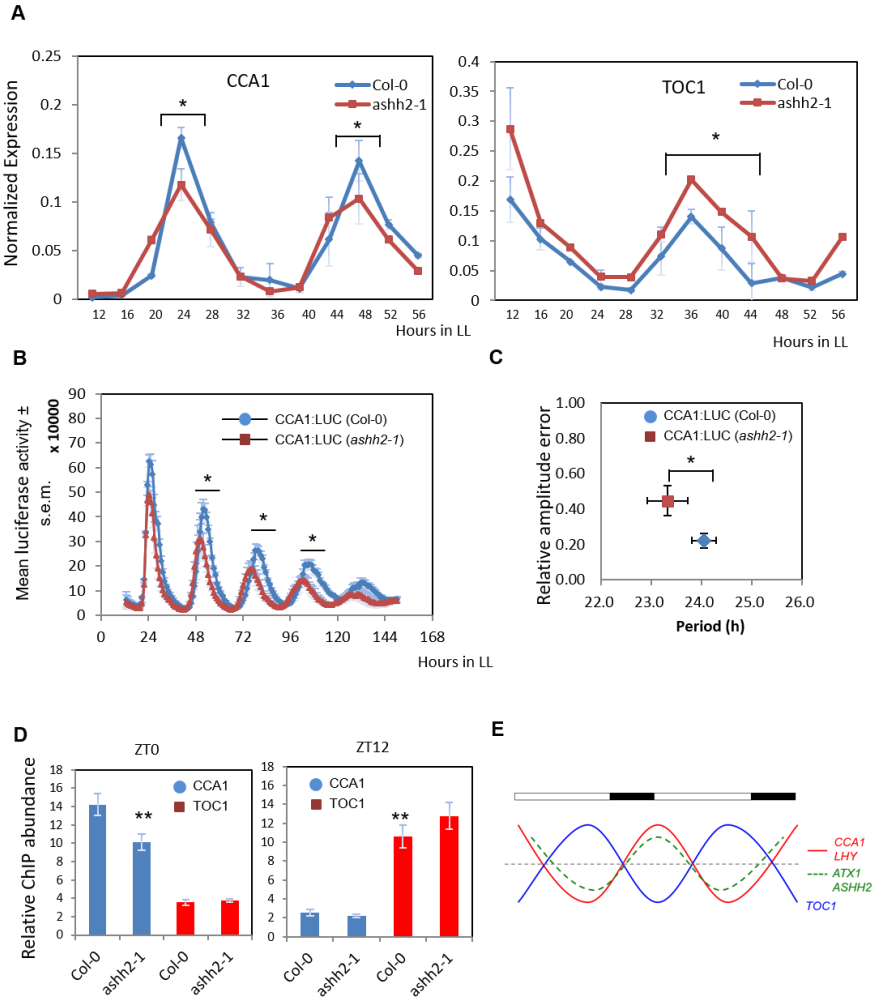

Figure 4: Histone methyltransferase mediates the periodicity and the amplitude of the clock. **(A)** Expression of CCA1 and TOC1 in wild-type Ws (wt) and ashh2-1 mutant seedlings growing in constant light (LL). mRNA levels were normalized to the expression of ACTIN7 . **(B)** Bioluminescence analysis of CCA1::LUC expression in T-DNA insertion line ashh2-1 and in wt. (n >25 seedlings per genotype) Wild-type (wt) traces correspond to CCA1::LUC seedlings. **(C)** Phase change of luciferase expression in wild-type CCA1::LUC (wt) and the ashh2-1 insertion lines shown in (B). Each symbol represents the normalized phase from n > 25 seedlings. **(D)** ChIP analysis of H3K4me3 accumulation in WT plants and in ashh2-1 mutants. Plants were grown under LD . Samples were analyzed at ZT0 and ZT12. H3K4me3 enrichment at the CCA1 and TOC1 promoters were normalized relative to the control ACTIN7. **(E)** Scheme depicting the combinatorial effect of chromatin marks accompanying the waveform of the oscillator genes.

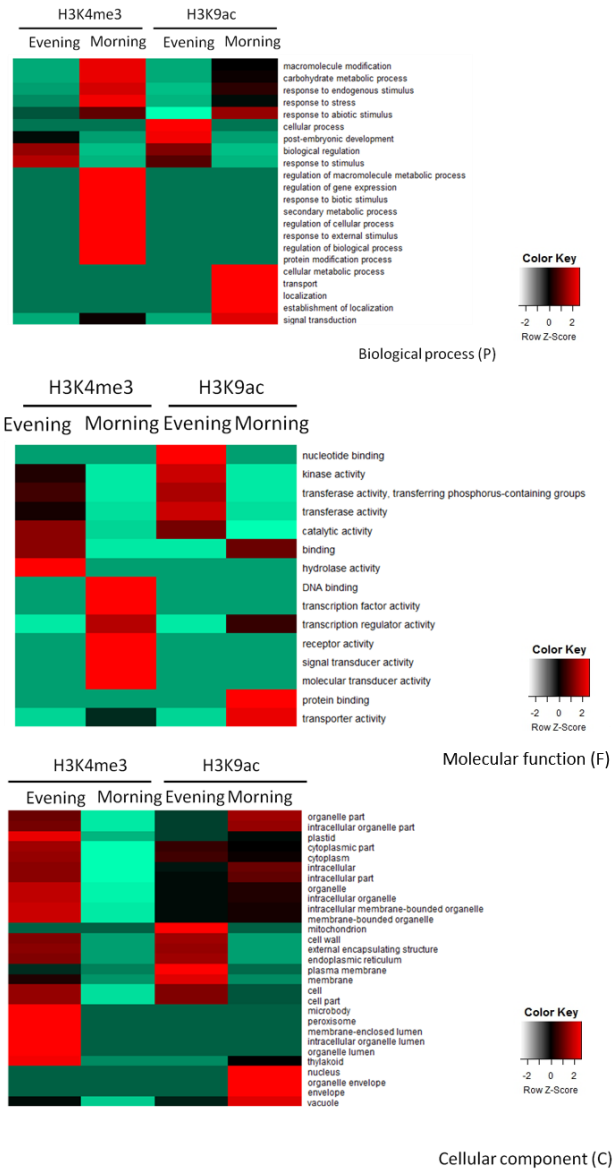

Figure 5: GO analysis of loci with cyclic H3K4me3 or H3K9ac binding signals. The color of each square represents the enrichment P value for the GO term.

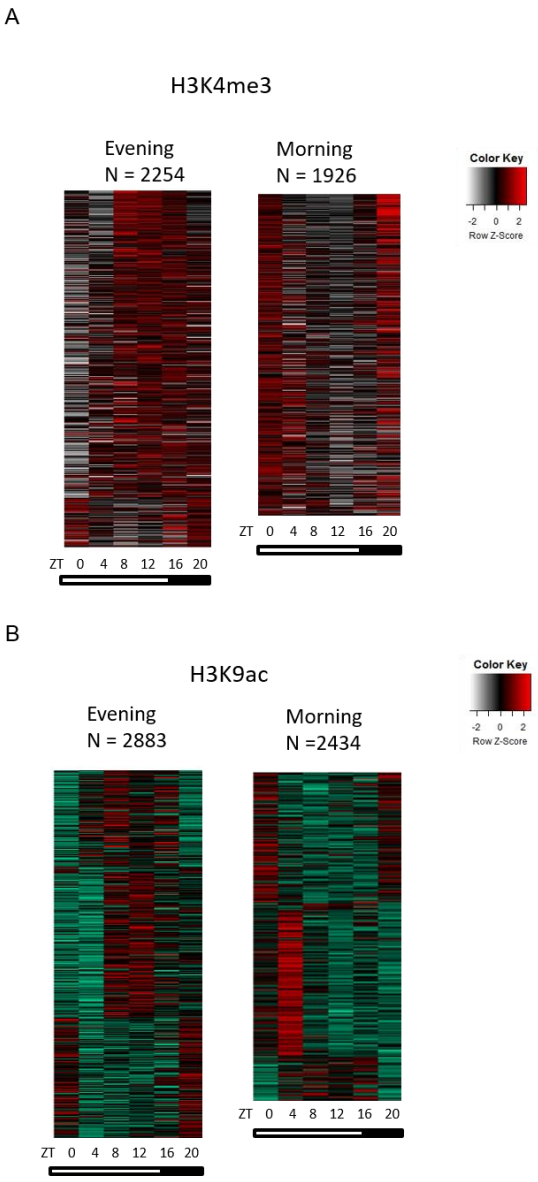

Figure 6: Transcriptome heat map of genes with cyclic H3K4me3 or H3K9ac binding signals. Cyclic binding was determined by JTK cycling ($p < 0.05$). The transcriptome data were pulled from the diurnal database. The signals are partitioned into the morning and evening clusters around medoids using R.

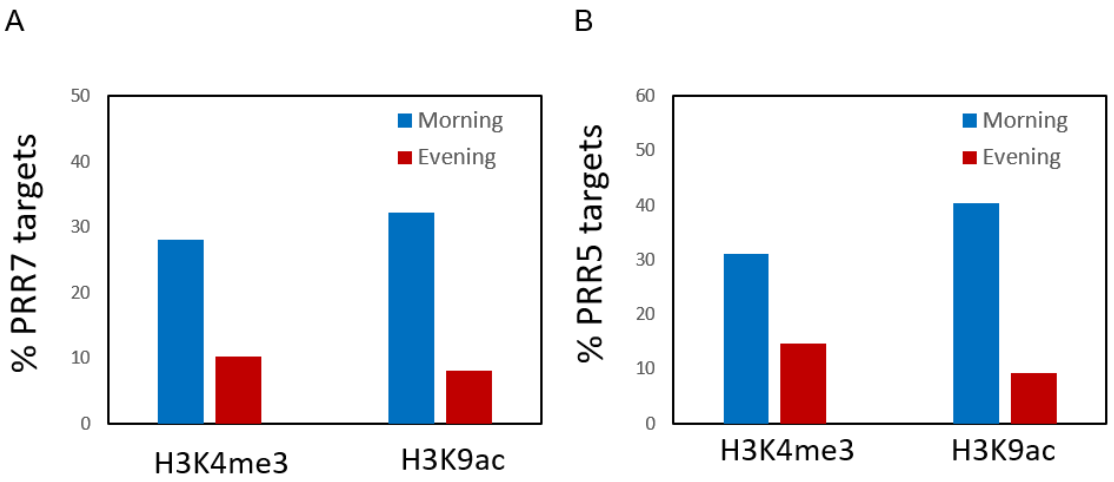

Figure 7: Percentage of PRR5 and PRR7 targets in genes with cyclic H3K4me3 or H3K9ac binding signals. (A) Bar graph of enrichment in PRR7 targets in loci with cyclic chromatin binding signals. PRR7 binding targets are pulled from previously published data set. Y axis is the percentage of PRR7 binding loci identified as having cyclic H3K4me3 or H3K9ac binding signals (B) Bar graph of enrichment in PRR5 targets in loci with cyclic chromatin binding signals.

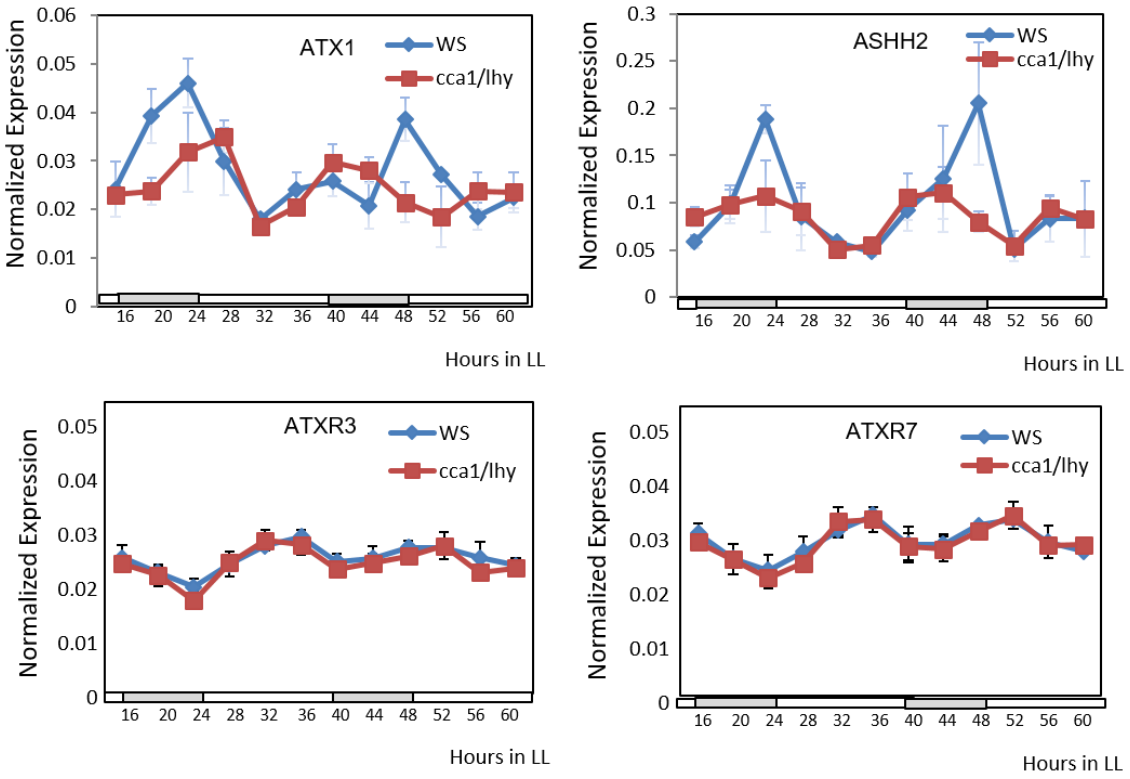

Figure 8: Expression of H3K4me3 methyltransferases in wild-type Ws (wt) and clock double mutant seedlings growing in constant light (LL). mRNA levels were normalized to the expression of ACTIN7. Three of the seven class III HMTase genes (ATX1/SDG27, ATXR7/SDG25, ATXR3/SDG2) and one of the class II HMTase gene (ASHH2/SDG8) have been shown to have H3K4me3 methyltransferase activity.

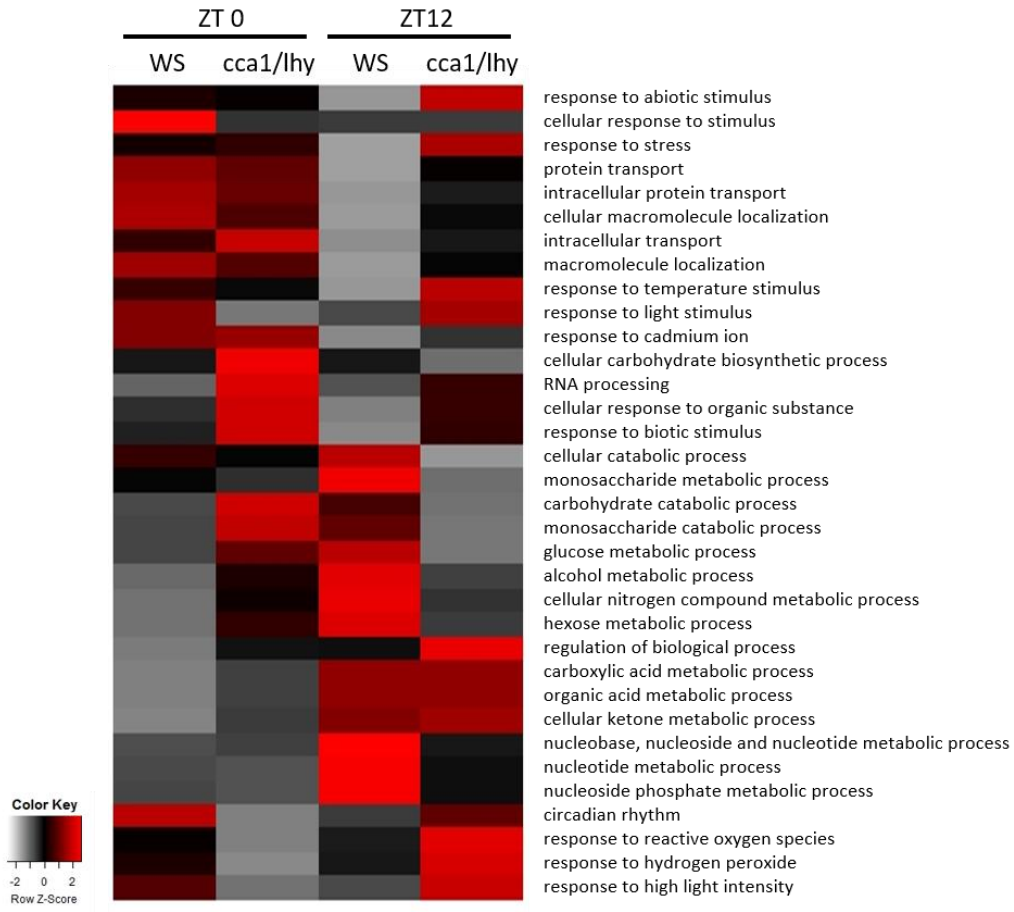

Figure 9: GO analysis of genes with differential H3H4me3 enrichment in wild-type Ws (wt) and clock double mutant at ZT0 and ZT12.

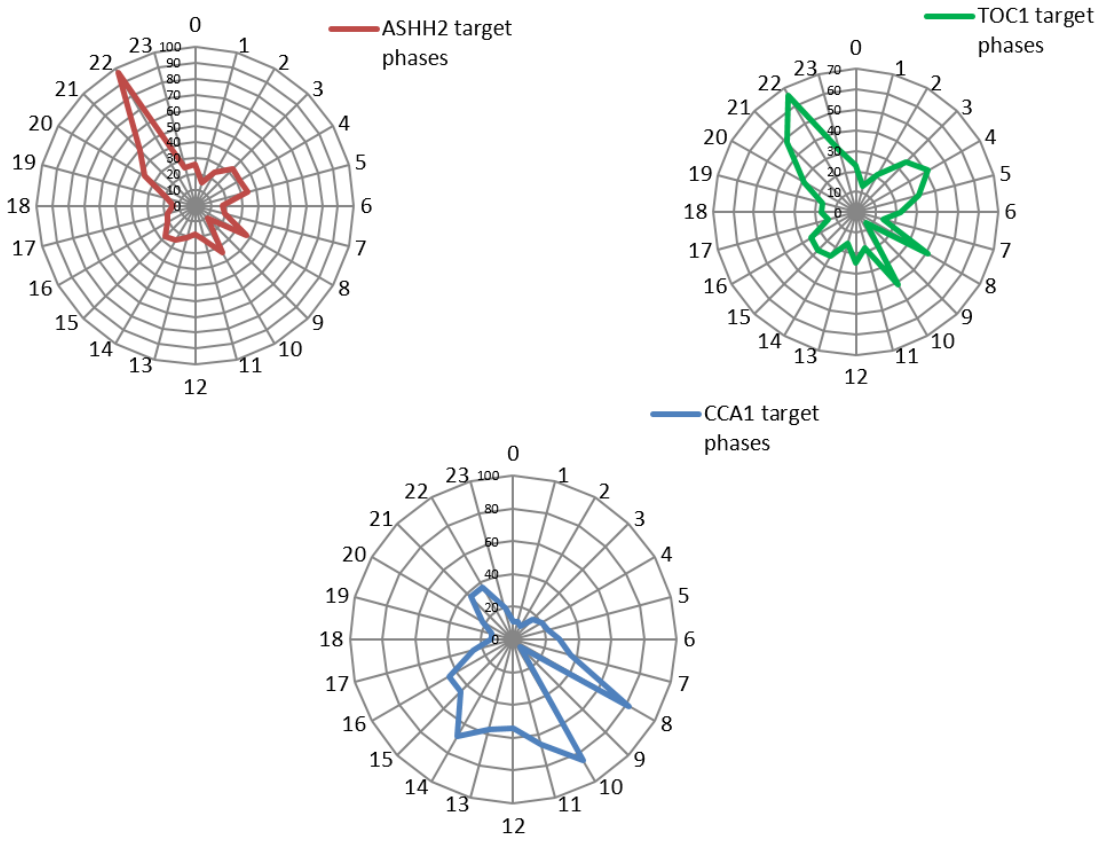

Figure 10: Phase distribution of ASHH2, CCA1 and TOC1 binding targets. ASHH2, CCA1, and TOC1 binding targets are pulled from previously published data set.

References

1. Masri, S. and P. Sassone-Corsi, *Plasticity and specificity of the circadian epigenome.* Nat Neurosci, 2010. **13**(11): p. 1324-1329.
2. Nakahata, Y., et al., *The NAD+-Dependent Deacetylase SIRT1 Modulates CLOCK-Mediated Chromatin Remodeling and Circadian Control.* Cell, 2008. **134**(2): p. 329-340.
3. Belden, W.J., J.J. Loros, and J.C. Dunlap, *Execution of the Circadian Negative Feedback Loop in Neurospora Requires the ATP-Dependent Chromatin-Remodeling Enzyme CLOCKSWITCH.* Molecular Cell, 2007. **25**(4): p. 587-600.
4. Ni, Z., et al., *Altered circadian rhythms regulate growth vigour in hybrids and allopolyploids.* Nature, 2009. **457**(7227): p. 327-331.
5. Crosio, C., et al., *Light induces chromatin modification in cells of the mammalian circadian clock.* Nat Neurosci, 2000. **3**(12): p. 1241-1247.
6. Etchegaray, J.-P., et al., *Rhythmic histone acetylation underlies transcription in the mammalian circadian clock.* Nature, 2003. **421**(6919): p. 177-182.
7. Ripperger, J.A. and U. Schibler, *Rhythmic CLOCK-BMAL1 binding to multiple E-box motifs drives circadian Dbp transcription and chromatin transitions.* Nat Genet, 2006. **38**(3): p. 369-374.
8. Doi, M., J. Hirayama, and P. Sassone-Corsi, *Circadian Regulator CLOCK Is a Histone Acetyltransferase.* Cell, 2006. **125**(3): p. 497-508.
9. Asher, G., et al., *SIRT1 Regulates Circadian Clock Gene Expression through PER2 Deacetylation.* Cell, 2008. **134**(2): p. 317-328.
10. Hirayama, J., et al., *CLOCK-mediated acetylation of BMAL1 controls circadian function.* Nature, 2007. **450**(7172): p. 1086-1090.
11. Brown, S.A., et al., *PERIOD1-Associated Proteins Modulate the Negative Limb of the Mammalian Circadian Oscillator.* Science, 2005. **308**(5722): p. 693.
12. Katada, S. and P. Sassone-Corsi, *The histone methyltransferase MLL1 permits the oscillation of circadian gene expression.* Nat Struct Mol Biol, 2010. **17**(12): p. 1414-1421.
13. Perales, M. and P. Más, *A Functional Link between Rhythmic Changes in Chromatin Structure and the Arabidopsis Biological Clock.* The Plant Cell, 2007. **19**(7): p. 2111-2123.
14. Farinas, B. and P. Mas, *Functional implication of the MYB transcription factor RVE8/LCL5 in the circadian control of histone acetylation.* The Plant Journal, 2011. **66**(2): p. 318-329.
15. Hemmes, H., et al., *Circadian Clock Regulates Dynamic Chromatin Modifications Associated with Arabidopsis CCA1/LHY and TOC1 Transcriptional Rhythms.* Plant and Cell Physiology, 2012. **53**(12): p. 2016-2029.
16. Malapeira, J., L.C. Khaitova, and P. Mas, *Ordered changes in histone modifications*

at the core of the Arabidopsis circadian clock. Proceedings of the National Academy of Sciences, 2012. **109**(52): p. 21540-21545.
17. Song, H.-R. and Y.-S. Noh, *Rhythmic Oscillation of Histone Acetylation and Methylation at the Arabidopsis Central Clock Loci.* Molecules and Cells, 2012. **34**(3): p. 279-287.
18. Seo, P.J. and P. Mas, *Multiple Layers of Posttranslational Regulation Refine Circadian Clock Activity in Arabidopsis.* The Plant Cell, 2014. **26**(1): p. 79-87.
19. Wang, L., J. Kim, and D.E. Somers, *Transcriptional corepressor TOPLESS complexes with pseudoresponse regulator proteins and histone deacetylases to regulate circadian transcription.* Proceedings of the National Academy of Sciences, 2013. **110**(2): p. 761-766.
20. Jones, M.A., et al., *Jumonji domain protein JMJD5 functions in both the plant and human circadian systems.* Proceedings of the National Academy of Sciences, 2010. **107**(50): p. 21623-21628.
21. Hughes, M.E., J.B. Hogenesch, and K. Kornacker, *JTK_CYCLE: an efficient non-parametric algorithm for detecting rhythmic components in genome-scale datasets.* Journal of biological rhythms, 2010. **25**(5): p. 372-380.
22. Koike, N., et al., *Transcriptional Architecture and Chromatin Landscape of the Core Circadian Clock in Mammals.* Science (New York, N.Y.), 2012. **338**(6105): p. 349-354.
23. Mockler, T.C., et al., *The Diurnal Project: Diurnal and Circadian Expression Profiling, Model-based Pattern Matching, and Promoter Analysis.* Cold Spring Harbor Symposia on Quantitative Biology, 2007. **72**: p. 353-363.
24. Malapeira, J., L.C. Khaitova, and P. Mas, *Ordered changes in histone modifications at the core of the Arabidopsis circadian clock.* Proceedings of the National Academy of Sciences of the United States of America, 2012. **109**(52): p. 21540-21545.
25. Nagel, D.H., et al., *Genome-wide identification of CCA1 targets uncovers an expanded clock network in Arabidopsis.* Proceedings of the National Academy of Sciences, 2015. **112**(34): p. E4802-E4810.
26. Huang, W., et al., *Circadian Clock Defines the Network Structure of the.* Science, 2012. **336**(6077): p. 75-79.
27. Nakamichi, N., et al., *Transcriptional repressor PRR5 directly regulates clock-output pathways.* Proceedings of the National Academy of Sciences of the United States of America, 2012. **109**(42): p. 17123-17128.
28. Kamioka, M., et al., *Direct Repression of Evening Genes by CIRCADIAN CLOCK-ASSOCIATED1 in the Arabidopsis Circadian Clock.* The Plant Cell, 2016. **28**(3): p. 696-711.
29. Valekunja, U.K., et al., *Histone methyltransferase MLL3 contributes to genome-scale circadian transcription.* Proceedings of the National Academy of Sciences, 2013. **110**(4): p. 1554-1559.

30. Fromm, M. and Z. Avramova, *ATX1/AtCOMPASS and the H3K4me3 marks: how do they activate Arabidopsis genes?* Current Opinion in Plant Biology, 2014. **21**: p. 75-82.
31. Pien, S., et al., *ARABIDOPSIS TRITHORAX1 Dynamically Regulates FLOWERING LOCUS C Activation via Histone 3 Lysine 4 Trimethylation.* The Plant Cell, 2008. **20**(3): p. 580-588.
32. Lee, S., et al., *Global Regulation of Plant Immunity by Histone Lysine Methyl Transferases.* The Plant Cell, 2016. **28**(7): p. 1640-1661.
33. Li, Y., et al., *The histone methyltransferase SDG8 mediates the epigenetic modification of light and carbon responsive genes in plants.* Genome Biology, 2015. **16**(1): p. 79.
34. Valencia-Morales, M.d.P., et al., *The Arabidopsis thaliana SET-domain-containing protein ASHH1/SDG26 interacts with itself and with distinct histone lysine methyltransferases.* Journal of Plant Research, 2012. **125**(5): p. 679-692.
35. Schuettengruber, B., et al., *Trithorax group proteins: switching genes on and keeping them active.* Nat Rev Mol Cell Biol, 2011. **12**(12): p. 799-814.
36. Miller, M., et al., *Natural variation in timing of stress-responsive gene expression predicts heterosis in intraspecific hybrids of Arabidopsis.* Nature Communications, 2015. **6**: p. 7453.
37. Clough, S.J. and A.F. Bent, *Floral dip: a simplified method forAgrobacterium-mediated transformation ofArabidopsis thaliana.* The Plant Journal, 1998. **16**(6): p. 735-743.
38. Ha, M., et al., *Coordinated histone modifications are associated with gene expression variation within and between species.* Genome Research, 2011. **21**(4): p. 590-598.
39. Bailey, T., et al., *Practical Guidelines for the Comprehensive Analysis of ChIP-seq Data.* PLoS Comput Biol, 2013. **9**(11): p. e1003326.
40. Koike, N., et al., *Transcriptional Architecture and Chromatin Landscape of the Core Circadian Clock in Mammals.* Science, 2012. **338**(6105): p. 349.
41. Zhang, Y., et al., *Model-based Analysis of ChIP-Seq (MACS).* Genome Biology, 2008. **9**(9): p. R137.
42. Du, Z., et al., *agriGO: a GO analysis toolkit for the agricultural community.* Nucleic Acids Research, 2010. **38**(suppl 2): p. W64-W70.
43. Michael, T.P. and C.R. McClung, *Phase-Specific Circadian Clock Regulatory Elements in Arabidopsis.* Plant Physiology, 2002. **130**(2): p. 627-638.
44. Haydon, M.J., et al., *Photosynthetic entrainment of the Arabidopsis thaliana circadian clock.* Nature, 2013. **502**(7473): p. 689-692.